



Thermodynamic Cycle Analysis of Magnetohydrodynamic–Bypass Hypersonic Airbreathing Engines

R.J. Litchford and J.W. Cole

Marshall Space Flight Center, Marshall Space Flight Center, Alabama

V.A. Bityurin

Institute of High Temperatures (IVTAN), Russian Academy of Science, Moscow, Russia

J.T. Lineberry

LyTEC, LLC, Tullahoma, Tennessee

National Aeronautics and
Space Administration

Marshall Space Flight Center • MSFC, Alabama 35812

Acknowledgments

The authors of this work acknowledge the support of the National Aeronautics and Space Administration (NASA), Space Transportation Directorate (STD), George C. Marshall Space Flight Center (MSFC). The results of the research reported herein were obtained at the request of the Space Transportation Directorate through the corroborative efforts of individuals associated with the Advanced Space Transportation Program Office (TD15/ASTP), MSFC; the Propulsion Research Center (TD40/PRC), MSFC; the Institute of High Temperatures (IVTAN), Russian Academy of Sciences, Moscow, Russia; and, LyTEC, LLC., Tullahoma, TN. The NASA Principal Investigator was Ron J. Litchford, TD40/PRC.

This technical publication has been reviewed and is approved.

George R. Schmidt
Deputy Manager
TD40/PRC
Marshall Space Flight Center

Gary M. Lyles
Manager
TD15/ASTP
Marshall Space Flight Center

Available from:

NASA Center for AeroSpace Information
7121 Standard Drive
Hanover, MD 21076-1320
(301) 621-0390

National Technical Information Service
5285 Port Royal Road
Springfield, VA 22161
(703) 487-4650

TABLE OF CONTENTS

1. INTRODUCTION	1
2. THERMODYNAMIC CYCLE ANALYSIS	3
2.1 Thermodynamic Cycle Description	3
2.2 Thermal Design Constraints	4
2.3 Basic Definitions	5
2.4 First Law Considerations	6
2.5 Second Law Considerations	9
2.6 System Thrust Characteristics	17
2.7 Ramjet Mode Mach Number Constraint	19
3. REPRESENTATIVE PERFORMANCE CALCULATIONS	20
3.1 Specific Thrust	20
3.2 Ramjet Mode Envelope	22
3.3 Stream Thrust Analysis	23
4. MAJOR TECHNICAL ISSUES	24
4.1 Air Ionization Considerations	24
4.2 MHD Technology Considerations	28
5. CONCLUSIONS	30
REFERENCES	31

LIST OF FIGURES

1.	Generic configuration of an airbreathing hypersonic engine with MHD-energy bypass system. Reference stations and process terminology are indicated. Also shown is the enthalpy-entropy process diagram for the generic MHD-bypass hypersonic airbreathing engine configuration	3
2.	Specific thrust characteristics as a function of flight Mach number for $\eta_{N(g)} = 0, 0.25, \text{ and } 0.5$ assuming $\eta_{s(g)} = \eta_{s(a)} = 0.9$ and $T_{0,\text{lim}} = 3000 \text{ K}$	21
3.	Maximum flight Mach number for maintaining subsonic combustion conditions as a function of the generator enthalpy extraction ratio. Assumes a maximum static burner entry temperature of $T_{3,\text{lim}} = 1600 \text{ K}$	22
4.	Naturally occurring interaction parameter behind a normal shock as a function of flight Mach number and altitude. Based on 1976 standard atmosphere and equilibrium air with molecular dissociation.	25
5.	Interaction parameter behind a normal shock as a function of flight Mach number for both unseeded and cesium-seeded equilibrium air. Calculations were performed for fixed altitudes of 100,000 and 125,000 ft.	26
6.	Hall parameter behind a normal shock as a function of flight Mach number for equilibrium air. Calculations were performed for fixed altitudes of 100,000 and 125,000 ft with $B = 1 \text{ T}$	28

LIST OF ACRONYMS

emf	electromotive force
HTSC	high-temperature superconductors
MHD	magnetohydrodynamic
TSFC	thrust-specific fuel consumption

ABBREVIATIONS AND SYMBOLS

0	stagnation condition, subscript
β	Hall parameter
γ	specific heat ratio
Δ	relative change
ε	electromotive force
η_c	combustion efficiency
η_N	enthalpy extraction/addition ratio
η_s	isentropic efficiency
π	exit-to-entrance stagnation pressure ratio
Π	global stagnation pressure ratio
ρ	density
σ	electrical conductivity
τ	exit-to-entrance stagnation temperature ratio
χ	fraction of generator power diverted to pre-ionizer
ψ	exit-to-entrance static temperature ratio
A	cross-sectional area
a	atmospheric condition; air; MHD accelerator; constant, subscript
B	magnetic field intensity
b	burner, subscript
C_p	constant pressure specific heat

ABBREVIATIONS AND SYMBOLS (Continued)

<i>d</i>	diffuser, subscript
<i>e</i>	expansion, subscript
ent	entrance condition, subscript
<i>F</i>	thrust
<i>f</i>	fuel-to-air mass flow ratio
<i>f</i>	fuel, subscript
<i>g</i>	MHD generator, subscript
<i>h</i>	enthalpy
<i>I_{sp}</i>	fuel specific impulse
<i>j</i>	current density
<i>L</i>	length
lim	limiting condition, subscript
<i>m</i>	mass flow rate
<i>M</i>	Mach number
<i>n</i>	nozzle, subscript
<i>p</i>	pressure
<i>p</i>	pre-ionizer, subscript
<i>Q</i>	MHD interaction parameter
<i>q_f</i>	fuel heating value
<i>R</i>	gas constant
<i>Sa</i>	stream thrust function
<i>T</i>	temperature
<i>u</i>	velocity
<i>w</i>	weight flow rate
<i>x</i>	reference condition, subscript

TECHNICAL PUBLICATION

THERMODYNAMIC CYCLE ANALYSIS OF MAGNETOHYDRODYNAMIC-BYPASS HYPERSONIC AIRBREATHING ENGINES

1. INTRODUCTION

Established analyses of conventional ramjet/scramjet performance characteristics indicate that a considerable decrease in efficiency can be expected at off-design flight conditions. This can be explained, in large part, by the deterioration of intake mass flow and limited inlet compression at low flight speeds and by the onset of thrust degradation effects associated with increased burner entry temperature at high flight speeds. In combination, these effects tend to impose lower and upper Mach number limits for practical flight. It has been noted, however, that magnetohydrodynamic (MHD) energy-management techniques represent a possible means for extending the flight Mach number envelope of conventional engines.¹⁻³ By transferring enthalpy between different stages of the engine cycle, it appears that the onset of thrust degradation may be delayed to higher flight speeds. Obviously, the introduction of additional process inefficiencies is inevitable with this approach, but it is believed that these losses are more than compensated through optimization of the combustion process.

The fundamental idea is to use MHD energy conversion processes to extract and bypass a portion of the intake kinetic energy around the burner. We refer to this general class of propulsion system as an MHD-bypass engine. In its generic configuration, an MHD generator is placed between the inlet and the burner as a means of converting flow kinetic energy into electrical power. In this way, the overall static temperature rise associated with inlet flow deceleration can be actively constrained, and the propulsion system is able to reach a higher freestream Mach number (i.e., higher inlet stagnation enthalpy) before the burner entry temperature exceeds the design limit. Furthermore, given a fixed limit for burner entry temperature, the inlet MHD generator can decelerate the flow to a lower velocity than that attainable using a simple adiabatic compression process. Thus, it is possible to increase the freestream Mach number for which the flow remains subsonic throughout the burner, and the ramjet mode can be sustained to much higher flight Mach numbers.

In this scheme, the inlet air must be ionized and have high electrical conductivity to attain effective MHD interaction in the generator. At moderate hypersonic Mach numbers of 12–18, it is possible to obtain the required levels of conductivity through equilibrium ionization of seeded air. However, at low hypersonic Mach numbers of 5–12, a fraction of the bypassed power must be diverted for operation of a nonequilibrium pre-ionizer. Therefore, inlet air ionization is a key technical issue with respect to practical viability.

Although the MHD-bypass engine concept is of considerable contemporary interest to the hypersonics community, a review of the open literature has revealed only a few analytical investigations aimed at performance prediction of these systems.⁴⁻⁹ These analyses demonstrate favorable performance characteristics under highly specific flight conditions, but a simplified thermodynamic cycle analysis would also be useful for the purpose of assessing systems performance potential on a more generalized basis.

This technical publication provides a brief description of a recently reported analysis assessing the performance potential and scientific feasibility of MHD-bypass hypersonic airbreathing engines using fundamental thermodynamic principles.¹⁰ The cycle analysis, based on a thermally and calorically perfect gas, incorporates strategically placed magnetohydrodynamic devices in the flow path and accounts for aerodynamic losses and thermodynamic process efficiencies in the various engine components. MHD device performance is completely described in terms of an enthalpy extraction/addition parameter and an isentropic efficiency. A provision is also made for diverting a fraction of the bypassed electrical power to an air pre-ionizer located at the inlet of the diffuser. The power consumed by the pre-ionizer is considered only as a variable parameter. The detailed ionization kinetics are not addressed in this paper. The analysis, while certainly not applicable to detailed performance analysis, is fundamental and is suitable as an indicator of potential performance gains associated with MHD energy bypass. It also reveals the flight Mach number range over which the system can effectively operate and suggests the range of component efficiencies needed for successful implementation.

The prime technical objective of this work was to find simple closed-form solutions for the performance of MHD-bypass airbreathing engines and use them to expose important trends and sensitivities, as well as to establish thermodynamic feasibility, without recourse to elaborate thermochemical calculations. From this standpoint, our methodology adheres to the analysis philosophy and spirit of Builder's pioneering approach.¹¹

2. THERMODYNAMIC CYCLE ANALYSIS

2.1 Thermodynamic Cycle Description

We consider the thermodynamic cycle of a hypersonic airbreathing engine of the ramjet/scramjet class that is augmented with an MHD energy management system. The geometrical configuration investigated here follows the generic MHD-bypass engine concept. The various engine components are shown in fig. 1 along with selected reference stations at critical axial positions along the engine flowpath. This figure also includes the entropy-enthalpy diagram for a modified Brayton cycle as represented by a sequence of eight process trajectories.

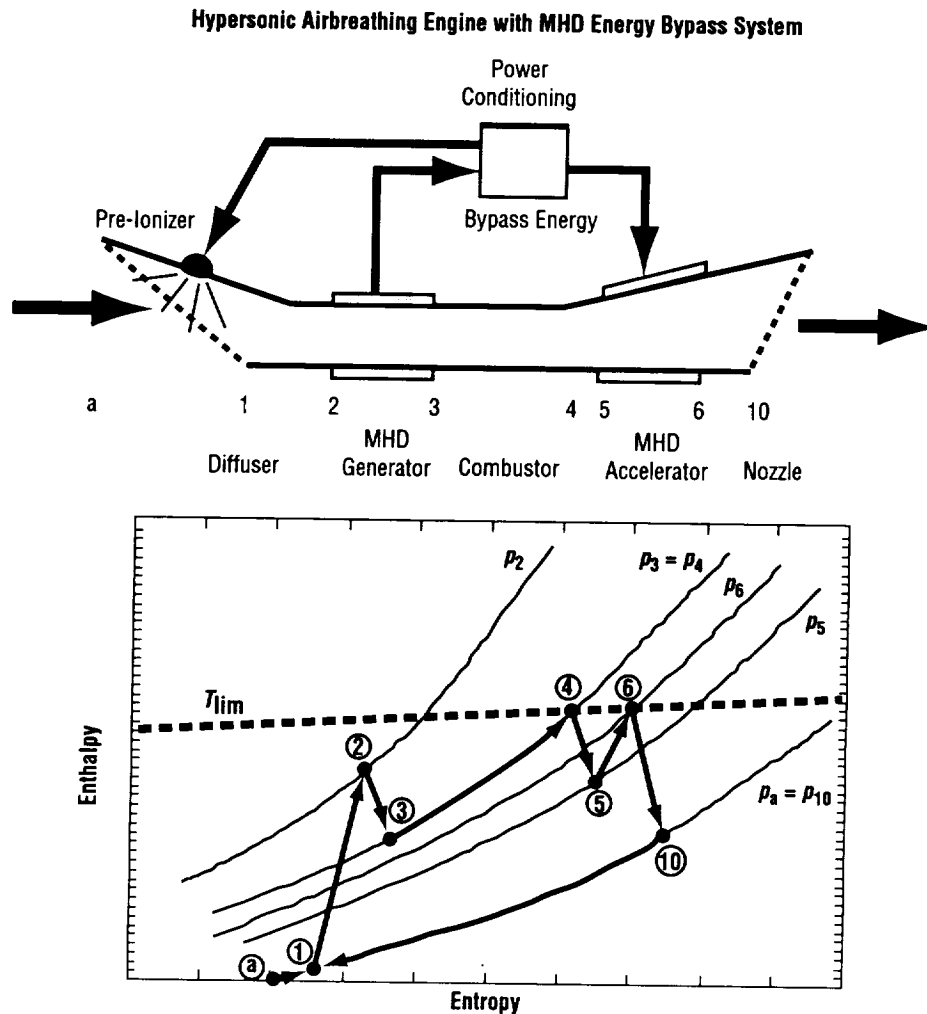


Figure 1. Generic configuration of a hypersonic airbreathing engine with MHD-energy bypass system. Reference stations and process terminology are indicated. Also shown is the enthalpy-entropy cycle diagram for the generic MHD-bypass hypersonic airbreathing engine configuration.

These process trajectories may be summarized as follows: (a→1) air pre-ionization and heat addition, (1→2) adiabatic compression and flow deceleration, (2→3) MHD conversion of total enthalpy to electrical power and deceleration of the flow, (3→4) constant static pressure and frictionless heat addition, (4→5) adiabatic expansion to prevent the temperature from exceeding design limits in the accelerator, (5→6) MHD conversion of electrical power to total flow enthalpy and acceleration of the flow, and (6→10) adiabatic expansion and acceleration of the exhaust flow.

2.2 Thermal Design Constraints

Presently, materials used for the walls of combustion chambers and nozzles cannot tolerate temperatures much above 1200 K. However, unlike gas turbine engines, the surfaces of ramjet/scramjet combustors can be kept much cooler than the main fluid stream by providing a shielding layer of relatively cool air near the wall. Therefore, this class of engine can accept higher peak burner temperatures and can operate at higher flight Mach numbers. In this way, the relative performance and operating range of ramjet/scramjet engines is greatly improved and extended over the gas turbine engine. As the flight Mach number continues to increase, however, the combustor inlet temperature also increases until, at some limiting Mach number, the peak cycle temperature begins to approach the temperature limit set by the wall materials and cooling methods. Because the heat energy added by fuel combustion can generate unacceptable temperature levels at the burner exit, we introduce a temperature design constraint on the peak combustor stagnation temperature in the form:

$$T_{0,4} \leq T_{0,\text{lim}} \quad (1)$$

Because the stagnation temperature is always increased in the MHD accelerator and this device is subject to similar thermal design limits as the burner, it is possible to introduce an additional design constraint on the peak accelerator temperature in the form:

$$T_{0,6} \leq T_{0,\text{lim}} \quad (2)$$

Even if material temperature limits could be extended, the static temperature at the burner entrance cannot be increased indefinitely. At temperatures approaching 2000 K, energy losses due to unequilibrated dissociation begin to impair performance and eventually overwhelm any benefits associated with increased cycle temperature. Based on the well-known thermodynamic characteristics of air, the maximum allowable burner entry temperature normally ranges from 1400–1700 K.¹² Therefore, a typical design value is ≈ 1600 K. For analysis purposes, we impose this practical thermodynamic constraint on design by requiring that the static temperature at the burner entrance not exceed a specified limiting value:

$$T_3 \leq T_{3,\text{lim}} \quad (3)$$

This limiting value should be low enough that air may be approximated as a thermally perfect gas with no dissociation effects during the entire inlet conditioning process.

2.3 Basic Definitions

To simplify the analysis, we assume that the working medium can be treated as a pure substance throughout the engine flow path and that the working medium is thermally and calorically perfect. Because practical aerodynamic (non-isentropic) losses can lead to significant entropy increases and stagnation pressure losses along the flow path, it is necessary to introduce various process efficiencies into the analysis. These efficiencies are introduced in terms of a stagnation pressure ratio ($\pi = p_{0,\text{exit}}/p_{0,\text{in}}$) for each engine process. Under these assumptions, it is possible to develop relations describing the thermodynamic process trajectories in each component of the engine and to reach a simple closed-form solution for fuel specific impulse (I_{sp}) and thrust-specific fuel consumption (TSFC).

We begin the development by specifying the freestream total temperature and total pressure in the stream tube of the engine inlet. These properties can be defined in terms of static conditions, which are altitude dependent, and the flight Mach number M_a using the following well-known gasdynamic relationships:

$$T_{0,a} = T_a \left(1 + \frac{\gamma - 1}{2} M_a^2 \right) \quad (4)$$

and

$$p_{0,a} = p_a \left(1 + \frac{\gamma - 1}{2} M_a^2 \right)^{\frac{\gamma}{\gamma - 1}} \quad (5)$$

where γ is the specific heat ratio. The objective is to track the variation in stagnation properties through the various engine components using the first and second laws of thermodynamics.

Before proceeding with the analysis, it is useful to note that any MHD device can be described in terms of two fundamental thermodynamic parameters: an enthalpy extraction/addition ratio (η_N) and an isentropic efficiency (η_s) which accounts for aerodynamic losses as well as joule-dissipation effects. The enthalpy extraction/addition ratio is defined as the ratio of the stagnation enthalpy change in the device to the entrance stagnation enthalpy:

$$\eta_N = \frac{\Delta h_0}{h_{0,\text{ent}}} \quad (6)$$

The isentropic efficiency represents the degree to which the actual process approaches an isentropic process. For a generator (energy extraction), it is defined as the ratio of the actual change in stagnation enthalpy to the ideal (isentropic) change in stagnation enthalpy that would accompany the same change in pressure:

$$\eta_{s(g)} = \frac{\Delta h_{0,\text{actual}}}{\Delta h_{0,\text{isentropic}}} \quad (7)$$

For an accelerator (energy insertion), it is defined as the ratio of the ideal to the actual:

$$\eta_{s(a)} = \frac{\Delta h_{0,isentropic}}{\Delta h_{0,actual}} \quad (8)$$

Note that the enthalpy extraction ratio and isentropic efficiency performance parameters fully define the operational characteristics of the generator and accelerator, including joule-dissipation losses. Representative values can be specified based on historical data from past MHD research.

2.4 First Law Considerations

The pre-ionizer takes a fraction (χ) of the energy produced by the MHD generator and introduces it to the inlet flow through an external energy addition process. The purpose is to increase the ionization level and electrical conductivity of the air before it enters the MHD generator. In the present formulation, we assume that no compression occurs in the pre-ionization region. Application of the first law of thermodynamics to the inlet stream tube in the pre-ionization region yields an energy balance in the form:

$$\dot{m}_a h_{0,1} = \dot{m}_a (h_{0,a} + \chi \eta_{N(g)} h_{0,2}) \quad (9)$$

where h_0 is the specific stagnation enthalpy, \dot{m}_a is the mass flow rate of air through the engine, and $\eta_{N(g)}$ is the enthalpy extraction ratio for the MHD generator. The quantity $\eta_{N(g)} h_{0,2}$ is the specific electrical energy extracted by the MHD generator. Since the flow is adiabatic in the diffuser, $h_{0,2} = h_{0,1}$, we can obtain the form:

$$\frac{T_{0,1}}{T_{0,a}} = \frac{h_{0,1}}{h_{0,a}} = \frac{1}{1 - \chi \eta_{N(g)}} \quad (10)$$

The compression process in the diffuser is assumed to be adiabatic such that the stagnation temperature remains invariant:

$$T_{0,2} = T_{0,1} = \frac{T_{0,a}}{1 - \chi \eta_{N(g)}} \quad (11)$$

By extracting flow enthalpy and converting it to electrical power, the MHD generator acts as an inlet flow conditioner for the engine. In the MHD generator, both total enthalpy and total pressure are decreased. Application of the first law of thermodynamics to the MHD generator yields an energy balance in the form:

$$\dot{m}_a h_{0,3} = \dot{m}_a (h_{0,2} - \eta_{N(g)} h_{0,2}) \quad (12)$$

where $\eta_{N(g)}h_{0,2}$ is the total enthalpy converted to electrical power per unit mass flow of air through the generator. In terms of stagnation temperatures, eq. (12) can be written in the form:

$$T_{0,3} = T_{0,2}(1 - \eta_{N(g)}) = T_{0,a} \frac{1 - \eta_{N(g)}}{1 - \chi\eta_{N(g)}} \quad (13)$$

Where we have introduced eq. (11) to obtain a result in terms of the freestream stagnation temperature.

In the burner, the stagnation temperature is increased as the chemical energy of the fuel is released as combustion heat. This process is assumed to occur at constant static pressure according to the assumed thermodynamic cycle although actual implementation might correspond more closely to burning in a constant-area duct. The energy equation applied to this idealized combustion process, neglecting the enthalpy of the incoming fuel, is

$$\begin{aligned} (\dot{m}_a + \dot{m}_f)h_{0,4} &= \dot{m}_a h_{0,3} + \eta_c \dot{m}_f q_f \\ (1 + f)h_{0,4} &= h_{0,3} + \eta_c f q_f \\ (1 + f)C_p T_{0,4} &= C_p T_{0,3} + \eta_c f q_f \end{aligned} \quad (14)$$

where \dot{m}_f represents the mass flow rate of fuel, q_f is the fuel heating value, η_c is the combustion efficiency of the burner, C_p is the constant pressure specific heat of the working fluid, and f is the fuel-to-air mass flow ratio. The combustion efficiency is included to account for the fact that some of the chemical energy of the fuel may not be released due to inadequate mixing or reaction time. The parameter may also be used to reflect energy losses associated with chemical dissociation. For constant specific heat, eq. (14) can be solved for the stagnation temperature at the burner exit:

$$T_{0,4} = \frac{T_{0,3} + (\eta_c f q_f / C_p)}{1 + f} \leq T_{0,\text{lim}} \quad (15)$$

Alternatively, eq. (14) can be solved for f in the form:

$$f = \frac{(T_{0,4}/T_{0,3}) - 1}{(\eta_c q_f / C_p T_{0,3}) - T_{0,4}/T_{0,3}} \quad (16)$$

where $T_{0,3}$ can be obtained from eq. (13). It should be apparent that the inequality of eq. (15) can be satisfied by limiting the value of $T_{0,3}$ through the extraction of enthalpy in the MHD generator and/or constraining the fuel-to-air ratio f such that

$$f \leq \frac{1 - (T_{0,3}/T_{0,\text{lim}})}{(\eta_c q_f / C_p T_{0,\text{lim}}) - 1} \quad (17)$$

A weak expansion component may be included after the burner to expand and cool the flow enough such that, after passage through the MHD accelerator, the static temperature remains below specified design limits. We assume that the expansion is adiabatic such that the stagnation temperature remains constant ($T_{0,5} = T_{0,4}$).

The MHD accelerator provides a mechanism for enthalpy addition in which the kinetic energy extracted from the inlet is recovered as an augmentation to overall engine thrust. In the accelerator, both total enthalpy and total pressure are increased.

Application of the first law of thermodynamics to the MHD accelerator yields an energy balance in the form:

$$\begin{aligned} (\dot{m}_a + \dot{m}_f)h_{0,6} &= (\dot{m}_a + \dot{m}_f)[h_{0,5} + \eta_{N(a)}h_{0,5}] \\ T_{0,6} &= T_{0,5}(1 + \eta_{N(a)}) \end{aligned} \quad (18)$$

where we have introduced the enthalpy addition ratio ($\eta_{N(a)}$). The product $\eta_{N(a)}h_{0,5}$ is the total enthalpy added to the flow per unit mass flow rate of combustion gases through the accelerator.

Because the electrical energy available for acceleration equals the total power produced by the generator minus that diverted for pre-ionization, $\eta_{N(a)}$ is directly related to the enthalpy extraction ratio of the generator according to the following power balance:

$$\eta_{N(a)}(\dot{m}_a + \dot{m}_f)h_{0,5} = (1 - \chi)\eta_{N(g)}\dot{m}_a h_{0,2} \quad (19)$$

or

$$\eta_{N(a)}T_{0,5} = \left(\frac{1}{1+f}\right)(1 - \chi)\eta_{N(g)}T_{0,1} \quad (20)$$

where we have used the fact that $T_{0,2}=T_{0,1}$. Upon substitution of eq. (20) into eq. (18) we eliminate $\eta_{N(a)}$ to obtain

$$T_{0,6} = T_{0,5} + \left(\frac{1}{1+f} \right) (1-\chi) \eta_{N(g)} T_{0,1} \quad (21)$$

Eliminating $T_{0,1}$ using eq. (10) and noting that $T_{0,5}=T_{0,4}$, we obtain the relation

$$T_{0,6} = T_{0,4} + \left(\frac{1}{1+f} \right) \frac{(1-\chi) \eta_{N(g)}}{1-\chi \eta_{N(g)}} T_{0,a} \quad (22)$$

The expansion process in the nozzle is assumed to be adiabatic such that the stagnation temperature remains invariant ($T_{0,10}=T_{0,6}$).

2.5 Second Law Considerations

As the propellant flows through the engine, irreversibilities result in an increase in entropy and a reduction in stagnation pressure. Therefore, real aerodynamic losses (or gains) may be accounted for through the introduction of a stagnation pressure ratio ($\pi = p_{0,\text{exit}}/p_{0,\text{in}}$) for each engine process. Expressions for these π parameters can be developed from fundamental thermodynamic and gasdynamic principles as demonstrated for conventional engine components by Heiser and Pratt¹² and for MHD devices by Bityurin et al.¹⁰ Because the π parameters for the MHD devices in the engine flow path introduce some novel considerations; however, we briefly develop the appropriate expressions for these components below.

2.5.1 Diffuser

The compression or diffuser efficiency $\eta_{s(d)}$ is defined as

$$\eta_{s(d)} = \frac{(\Delta h)_{\text{isentropic}}}{(\Delta h)_{\text{actual}}} = \frac{h_2 - h_x}{h_2 - h_1} \leq 1 \quad (23)$$

where h_x is the enthalpy at the inlet necessary to achieve the same static pressure rise in an isentropic compression process. Equation (23) may also be written in the form:

$$\eta_{s(d)} = \frac{h_2 - h_x}{h_2 - h_1} = \frac{\psi_d - \frac{T_x}{T_1}}{\psi_d - 1} \quad (24)$$

or

$$\frac{T_x}{T_1} = \psi_d(1 - \eta_{s(d)}) + \eta_{s(d)} \quad (25)$$

Here, we have introduced the diffuser static temperature ratio $\psi_d = T_2/T_1$ as a new independent variable.

Applying Gibbs equation for the idealized isentropic compression process yields

$$\frac{dp}{p} = \frac{C_p}{R} \frac{dT}{T} = \left(\frac{\gamma}{\gamma - 1} \right) \frac{dT}{T} \quad (26)$$

Thus, integration of eq. (26) through the diffuser gives

$$\frac{p_2}{p_1} = \left(\frac{T_2}{T_x} \right)^{\frac{\gamma}{\gamma - 1}} = \left(\psi_d \frac{T_1}{T_x} \right)^{\frac{\gamma}{\gamma - 1}} \quad (27)$$

Equations (25) and (27) can now be combined to eliminate the ratio T_1/T_x . The result is an expression for the diffuser static pressure ratio:

$$\frac{p_2}{p_1} = \left(\frac{\psi_d}{\psi_d(1 - \eta_{s(d)}) + \eta_{s(d)}} \right)^{\frac{\gamma}{\gamma - 1}} \quad (28)$$

Now, by using the Mach number relation between the stagnation and static pressures, we can write the stagnation pressure ratio for the diffuser in the form:

$$\pi_d = \frac{p_{0,2}}{p_{0,1}} = \frac{p_2}{p_1} \left\{ \frac{1 + \frac{\gamma - 1}{2} M_2^2}{1 + \frac{\gamma - 1}{2} M_1^2} \right\}^{\frac{\gamma}{\gamma - 1}} \quad (29)$$

Since the total temperature is conserved, we can also use the Mach number relation between the stagnation and static temperatures to obtain the following expression for ψ_d :

$$\psi_d = \frac{T_2}{T_1} = \left\{ \frac{1 + \frac{\gamma-1}{2} M_1^2}{1 + \frac{\gamma-1}{2} M_2^2} \right\} \quad (30)$$

Combining eq. (29) and eq. (30) gives

$$\pi_d = \frac{p_2}{p_1} \left(\frac{1}{\psi_d} \right)^{\frac{\gamma}{\gamma-1}} \quad (31)$$

Finally, eq. (28) can be substituted into eq. (31) to obtain the desired result for the stagnation pressure ratio in the diffuser:

$$\pi_d = \left(\frac{1}{\psi_{d,\text{lim}}(1 - \eta_{s(d)}) + \eta_{s(d)}} \right)^{\frac{\gamma}{\gamma-1}} \quad (32)$$

where we now indicate a limiting value for the static temperature ratio.

2.5.2 MHD Generator

Consider the MHD generator in which the stagnation pressure must decrease. We begin with the Gibbs equation for an ideal (isentropic) process as applied to stagnation properties

$$\frac{dp_0}{p_0} = \frac{\gamma}{\gamma-1} \frac{dh_0}{h_0} \quad (33)$$

and integrate through the generator to obtain the stagnation pressure ratio in terms of the total enthalpy ratio:

$$\pi_g = \frac{p_{0,3}}{p_{0,2}} = \left(\frac{h_{0,3}}{h_{0,2}} \right)^{\frac{\gamma}{\gamma-1}} \quad (34)$$

Utilizing the definition of $\eta_{N(g)}$ given by eq. (6) and the definition of $\eta_{s(g)}$ given by eq. (7), we can form the following relationship between generator performance parameters:

$$\begin{aligned}\frac{\eta_{N(g)}}{\eta_{s(g)}} &= \frac{(h_{0,2} - h_{0,3})_{isentropic} (h_{0,2} - h_{0,3})_{actual}}{(h_{0,2} - h_{0,3})_{actual} h_{0,2}} \\ &= \left(\frac{h_{0,2} - h_{0,3}}{h_{0,2}} \right)_{isentropic} \\ &= 1 - \left(\frac{h_{0,3}}{h_{0,2}} \right)_{isentropic}\end{aligned}\quad (35)$$

Upon substituting eq. (35) into eq. (34), we obtain the desired expression for the stagnation pressure ratio in the MHD generator:

$$\pi_g = \frac{p_{0,3}}{p_{0,2}} = \left(1 - \frac{\eta_{N(g)}}{\eta_{s(g)}} \right)^{\frac{\gamma}{\gamma-1}} \quad (36)$$

2.5.3 Burner

Because of the heat addition occurring in the burner, there is an increase in entropy and a corresponding loss in total pressure. This drop in total pressure is a direct manifestation of Rayleigh heating loss which obeys the following differential relationship:

$$\frac{dp_0}{p_0} = -\frac{\gamma}{2} M^2 \frac{dT_0}{T_0} \quad (37)$$

For constant pressure heating in the burner, the Rayleigh heating loss law leads to the following expression for the stagnation pressure ratio in the burner¹² (pp. 77–80 of the reference):

$$\pi_b = \frac{p_{0,4}}{p_{0,3}} = \left[1 + \frac{\gamma-1}{2} M_3^2 \left(1 - \frac{1}{\tau_b} \right) \right]^{-\frac{\gamma}{\gamma-1}} \quad (38)$$

where $\tau_b = T_{0,4}/T_{0,3}$ is the stagnation temperature ratio in the burner. The value of the burner entry Mach number M_3 depends upon the design configuration of the MHD generator.

2.5.4 Cooling Expansion

A weak expansion component may be included after the burner to expand and cool the flow enough such that, after passage through the MHD accelerator, the static temperature remains below specified design limits. Because the degree of expansion would be very low, we anticipate that π_e would take on a value very close to unity.

Assuming adiabatic expansion, the stagnation temperature remains constant throughout the nozzle. Because of departures from isentropic behavior, however, stagnation pressure losses will occur. These losses may be expressed in terms of an expansion efficiency defined as

$$\eta_{s(e)} = \frac{(\Delta h)_{actual}}{(\Delta h)_{isentropic}} = \frac{h_4 - h_5}{h_4 - h_y} \leq 1 \quad (39)$$

where h_y is the static enthalpy at the end of expansion necessary to achieve the same static pressure drop in an isentropic process. In reality, the process depends upon flight conditions, but this approach is sufficient within the assumptions of our analysis. Equation (39) may also be written in the form:

$$\eta_{s(e)} = \frac{h_4 - h_5}{h_4 - h_y} = \frac{1 - (T_5/T_4)}{1 - (T_y/T_4)} \quad (40)$$

which may be solved for T_y/T_4

$$\frac{T_y}{T_4} = \frac{\psi_e - 1}{\eta_{s(e)}} + 1 \quad (41)$$

where we have introduced the static temperature ratio for the expansion as $\psi_e = T_5/T_4$. Gibbs equation for the idealized isentropic expansion process is

$$\frac{dp}{p} = \left(\frac{\gamma}{\gamma - 1} \right) \frac{dT}{T} \quad (42)$$

and integration of eq. (42) through the expansion gives

$$\frac{p_5}{p_4} = \frac{p_y}{p_4} = \left(\frac{T_y}{T_4} \right)^{\frac{\gamma}{\gamma - 1}} \quad (43)$$

Substitution of eq. (41) into eq. (43) eliminates T_y/T_4

$$\frac{p_5}{p_4} = \left(\frac{\psi_e - 1}{\eta_{s(e)}} + 1 \right)^{\frac{\gamma}{\gamma-1}} \quad (44)$$

Using the Mach number relation between stagnation and static pressures, we can write the stagnation pressure ratio for the expansion in the form:

$$\pi_e = \frac{p_{0,5}}{p_{0,4}} = \frac{p_5}{p_4} \left\{ \frac{1 + \frac{\gamma-1}{2} M_5^2}{1 + \frac{\gamma-1}{2} M_4^2} \right\}^{\frac{\gamma}{\gamma-1}} \quad (45)$$

Using the Mach number relation between stagnation and static temperatures, we can write the stagnation temperature ratio for the expansion in the form:

$$\frac{T_{0,5}}{T_{0,4}} = \frac{T_5}{T_4} \frac{1 + \frac{\gamma-1}{2} M_5^2}{1 + \frac{\gamma-1}{2} M_4^2} \quad (46)$$

But the total temperature is conserved, and eq. (46) can be written in terms of ψ_e :

$$\psi_e = \frac{T_5}{T_4} = \frac{1 + \frac{\gamma-1}{2} M_4^2}{1 + \frac{\gamma-1}{2} M_5^2} \quad (47)$$

Combining eq. (47) and eq. (45), we therefore deduce

$$\pi_e = \frac{p_{0,5}}{p_{0,4}} = \frac{p_5}{p_4} \left(\frac{1}{\psi_e} \right)^{\frac{\gamma}{\gamma-1}} \quad (48)$$

Upon substituting for p_5/p_4 using eq. (43), we obtain the desired final result for the stagnation pressure ratio:

$$\pi_e = \frac{p_{0,5}}{p_{0,4}} = \left(\frac{\psi_e - 1}{\eta_{s(e)} \psi_e} + \frac{1}{\psi_e} \right)^{\frac{\gamma}{\gamma-1}} \quad (49)$$

2.5.5 MHD Accelerator

Consider, now, the MHD accelerator in which the stagnation pressure must increase. We begin with the Gibbs equation for an ideal (isentropic) process as applied to stagnation properties and integrate through the accelerator to obtain the stagnation pressure ratio in terms of the total enthalpy ratio:

$$\pi_a = \frac{p_{0,6}}{p_{0,5}} = \left(\frac{h_{0,6}}{h_{0,5}} \right)^{\frac{\gamma}{\gamma-1}} \quad (50)$$

Utilizing the definition of $\eta_{N(a)}$ given by eq. (6) and the definition of $\eta_{s(a)}$ given by eq. (8), we can form the following relationship between accelerator performance parameters:

$$\begin{aligned} \eta_{N(a)} \eta_{s(a)} &= \frac{(h_{0,6} - h_{0,5})_{isentropic}}{(h_{0,6} - h_{0,5})_{actual}} \frac{(h_{0,6} - h_{0,5})_{actual}}{h_{0,5}} \\ &= \left(\frac{h_{0,6} - h_{0,5}}{h_{0,5}} \right)_{isentropic} \\ &= \left(\frac{h_{0,6}}{h_{0,5}} \right)_{isentropic} - 1 \end{aligned} \quad (51)$$

Upon substituting eq. (51) into eq. (50), we obtain an expression for the stagnation pressure ratio in the MHD accelerator in terms of the thermodynamic parameters of the device

$$\pi_a = \frac{p_{0,6}}{p_{0,5}} = \left(1 + \eta_{N(a)} \eta_{s(a)} \right)^{\frac{\gamma}{\gamma-1}} \quad (52)$$

If we eliminate $\eta_{N(a)}$ using eq. (20) and eliminate $T_{0,1}$ using eq. (10), we obtain the desired final expression for the stagnation pressure ratio in the MHD accelerator

$$\pi_a = \frac{p_{0,6}}{p_{0,5}} = \left[1 + \eta_{s(a)} \left(\frac{1}{1+f} \right) \frac{(1-\chi)\eta_{N(g)} T_{0,a}}{1-\chi\eta_{N(g)} T_{0,4}} \right]^{\frac{\gamma}{\gamma-1}} \quad (53)$$

where we have also used $T_{0,5}=T_{0,4}$.

2.5.6 Nozzle

The irreversible losses in the nozzle are accounted for in terms of a nozzle expansion efficiency in the same form as defined for the cooling expansion in eq. (39):

$$\eta_{s(n)} = \frac{(\Delta h)_{actual}}{(\Delta h)_{isentropic}} = \frac{h_6 - h_{10}}{h_6 - h_y} \leq 1 \quad (54)$$

Thus, the relationships derived for the cooling expansion directly apply to the nozzle with appropriate modifications to the engine station references. For instance, when the form of eq. (48) is applied to the nozzle expansion process, we obtain

$$\pi_n = \frac{p_{0,10}}{p_{0,6}} = \frac{p_{10}}{p_6} \left(\frac{1}{\psi_n} \right)^{\frac{\gamma}{\gamma-1}} \quad (55)$$

where $\psi_n = T_{10}/T_6$ is the static temperature ratio of the nozzle. In this case, however, it is advantageous to express the stagnation pressure ratio in terms of the nozzle static pressure ratio rather than the nozzle static temperature ratio (ψ_n). This can be done by applying the form of eq. (44) to the nozzle, solving for ψ_n , and using this result to eliminate ψ_n in eq. (55). This yields the following form for π_n :

$$\pi_n = \left[\eta_{s(n)} + (1 - \eta_{s(n)}) \left(\frac{p_6}{p_{10}} \right)^{(\gamma-1)/\gamma} \right]^{\frac{-\gamma}{\gamma-1}} \quad (56)$$

2.6 System Thrust Characteristics

There is now sufficient information to compute the total engine thrust including the effect of aerodynamic losses. Although the π parameters are not truly constant over large Mach number variations and γ can vary significantly through the engine flowpath, the following development demonstrates the essential performance characteristics of hypersonic airbreathing engines.

First, we utilize the Mach number relation between stagnation and static pressures as defined by eq. (5) and evaluate these expressions at the inlet and exit of the engine. We then form the ratio between these expressions and solve for the exit Mach number M_e^2 :

$$M_e^2 = \frac{2}{\gamma - 1} \left[\left(1 + \frac{\gamma - 1}{2} M_a^2 \right) \left(\frac{p_{0,e} p_a}{p_{0,a} p_e} \right)^{(\gamma-1)/\gamma} - 1 \right] \quad (57)$$

but

$$\frac{p_{0,e}}{p_{0,a}} = \frac{p_{0,1}}{p_{0,a}} \frac{p_{0,2}}{p_{0,1}} \frac{p_{0,3}}{p_{0,2}} \frac{p_{0,4}}{p_{0,3}} \frac{p_{0,5}}{p_{0,4}} \frac{p_{0,6}}{p_{0,5}} \frac{p_{0,10}}{p_{0,6}} = \pi_p \pi_d \pi_g \pi_b \pi_e \pi_a \pi_n \quad (58)$$

where π_p , π_d , π_g , π_b , π_e , π_a , and π_n are the π parameters for the pre-ionizer, diffuser, generator, burner, cooling expansion, accelerator, and nozzle, respectively. Thus, in terms of the component stagnation pressure ratios

$$M_e^2 = \frac{2}{\gamma - 1} \left[\left(1 + \frac{\gamma - 1}{2} M_a^2 \right) \left(\pi_p \pi_d \pi_g \pi_b \pi_e \pi_a \pi_n \frac{p_a}{p_e} \right)^{(\gamma-1)/\gamma} - 1 \right] \quad (59)$$

We now define a global stagnation pressure ratio parameter Π as

$$\Pi = \left(1 + \frac{\gamma - 1}{2} M_a^2 \right) \left(\pi_p \pi_d \pi_g \pi_b \pi_e \pi_a \pi_n \frac{p_a}{p_e} \right)^{(\gamma-1)/\gamma} \quad (60)$$

such that

$$M_e^2 = \frac{2}{\gamma - 1} [\Pi - 1] \quad (61)$$

Assuming that heat transfer from the engine is negligible, the exhaust velocity is given by $u_e = M_e \sqrt{\gamma R T_e}$ or, in terms of the exhaust stagnation temperature

$$u_e = M_e \sqrt{\gamma R T_{0,6} / \left(1 + \frac{\gamma - 1}{2} M_e^2\right)} \quad (62)$$

where we have made use of the fact that $T_{0,10} = T_{0,6}$. The fuel-air ratio necessary to produce the desired value for $T_{0,4}$ is given by eq. (16).

The thrust for a hypersonic airbreathing engine is defined by

$$F = (\dot{m}_a + \dot{m}_e)u_e - \dot{m}_a u_a + (p_e - p_a)A_e \quad (63)$$

and the thrust per unit mass flow rate of air becomes

$$\frac{F}{\dot{m}_a} = [(1 + f)u_e - u_a] + \frac{1}{\dot{m}_a} (p_e - p_a)A_e \quad (64)$$

Substituting eq. (62) into eq. (64) yields the desired form:

$$\frac{F}{\dot{m}_a} = \left[(1 + f) \sqrt{\frac{2\gamma R T_{0,6} (\Pi - 1)}{(\gamma - 1)\Pi}} - M_a \sqrt{\gamma R T_a} \right] + \frac{p_e A_e}{\dot{m}_a} \left(1 - \frac{p_a}{p_e} \right) \quad (65)$$

where $T_{0,6}$ is obtained from eq. (22) using $T_{0,4}$ (i.e., $T_{0,\text{lim}}$) as a parameter. The fuel specific impulse may also be determined as

$$I_{sp} = \frac{F}{\dot{w}_f} = \frac{F/\dot{w}_a}{f} \quad (66)$$

where \dot{w}_a and \dot{w}_f are the weight flow rates of air and fuel, respectively. Following conventional practice, the TSFC is defined as the ratio of fuel mass flow rate to engine thrust:

$$TSFC = \frac{\dot{m}_f}{F} = \frac{f}{F/\dot{m}_a} \quad (67)$$

2.7 Ramjet Mode Mach Number Constraint

The limitation on burner entry temperature leads directly to a restriction on the burner entry Mach number M_3 . That is, the flow can be decelerated only a limited amount before the static temperature at the burner inlet becomes too great for effective combustion, and at some particular flight Mach number, it becomes necessary to transition to a supersonic combustion mode ($M_3 > 1$). For the MHD-bypass engine configuration, however, the burner entry temperature is affected by the enthalpy extraction process in the MHD generator. Indeed, the bypassing of flow enthalpy around the burner enables the vehicle to obtain a higher flight Mach number while maintaining a subsonic combustion mode.

We can easily develop a relation for the burner entry Mach number as a function of the flight Mach number, the enthalpy extraction ratio, and the static temperature limit. We begin with the Mach number relation between stagnation temperature and static temperature at the burner entrance

$$T_{0,3} = T_3 \left(1 + \frac{\gamma - 1}{2} M_3^2 \right) \quad (68)$$

Then we eliminate $T_{0,3}$ using eq. (13) while enforcing a burner entry static temperature limit ($T_{3,\text{lim}}$) and find that the burner entry Mach number is given by

$$M_3 = \sqrt{\frac{2}{\gamma - 1} \left[\frac{T_a}{T_{3,\text{lim}}} \frac{1 - \eta_{N(g)}}{1 - \chi \eta_{N(g)}} \left(1 + \frac{\gamma - 1}{2} M_a^2 \right) - 1 \right]} \quad (69)$$

This relation implies definite operating restrictions. For example, when

$$M_a < \sqrt{\frac{2}{\gamma - 1} \left(\frac{T_{3,\text{lim}}}{T_a} \frac{1 - \chi \eta_{N(g)}}{1 - \eta_{N(g)}} - 1 \right)} \quad (70)$$

no solution is physically possible since $T_{3,\text{lim}}$ would exceed the stagnation temperature of the freestream flow. Furthermore, when

$$M_a > \sqrt{\frac{2}{\gamma - 1} \left[\left(\frac{\gamma + 1}{2} \right) \frac{T_{3,\text{lim}}}{T_a} \frac{1 - \chi \eta_{N(g)}}{1 - \eta_{N(g)}} - 1 \right]} \quad (71)$$

the flow entering the burner must remain supersonic or $T_{3,\text{lim}}$ will be exceeded.

3. REPRESENTATIVE PERFORMANCE CALCULATIONS

3.1 Specific Thrust

It is instructive to compare the performance of an MHD-bypass hypersonic airbreathing engine with that of a conventional ramjet system. For this purpose, Hill and Peterson's well-known analysis for a nonideal ramjet represents a suitable baseline case.¹³ Indeed, their analytical results are directly recoverable from our development by simply eliminating all MHD interaction (i.e., setting $\eta_{N(g)}=\eta_{N(a)}=0$). Following Hill and Peterson, we assumed a freestream temperature of $T_a=220$ K and used the thermodynamic properties of air throughout the engine flow path. The fuel heat of combustion was taken to be $q_f=45\times 10^3$ kJ/kg with 100 percent combustion efficiency and a stagnation temperature limit was enforced at the burner exit. As in Hill and Peterson's case, we considered constant stagnation pressure ratios of $\pi_d=0.7$, $\pi_b=0.95$, and $\pi_n=0.98$ for the diffuser, burner, and nozzle, respectively. As previously noted, the calculations are limited because γ is not constant throughout the engine flowpath and the stagnation pressure ratios are not independent of flight Mach number. These coefficients were taken as constants solely for the purpose of maintaining simplicity and clarity. We have optimistically assumed that $\eta_{s(g)}=\eta_{s(a)}=0.9$ and computed π_g (loss) and π_a (gain) using eq. (25) and eq. (28), respectively. The power needed to drive the pre-ionizer is difficult to estimate at this juncture and we utilized a value of $\chi=0.05$ for demonstration purposes.

The computed specific thrust is shown as a function of flight Mach number in fig. 2 for enthalpy extraction ratios of $\eta_{N(g)}=0, 0.25$, and 0.5 and a maximum burner stagnation temperature of 3000 K. The case without any MHD interaction corresponds directly with Hill and Peterson's results and is demonstrative of a conventional hypersonic airbreathing engine. The specific thrust in this instance peaks at a flight Mach number between 2 and 3 after which it steadily decreases to zero near $M_a=8$. The results with MHD interaction demonstrate a reduction in peak performance and a shifting of the specific thrust curve to higher flight Mach numbers. The loss in performance using MHD-bypass is due to increased non-isentropic losses associated with the MHD energy conversion devices. However, the ability to bypass flow enthalpy around the burner permits optimization of the combustion process at higher flight Mach numbers and enables the production of thrust in a flight regime not obtainable with conventional engines. This capability is the primary advantage of the MHD-bypass concept.

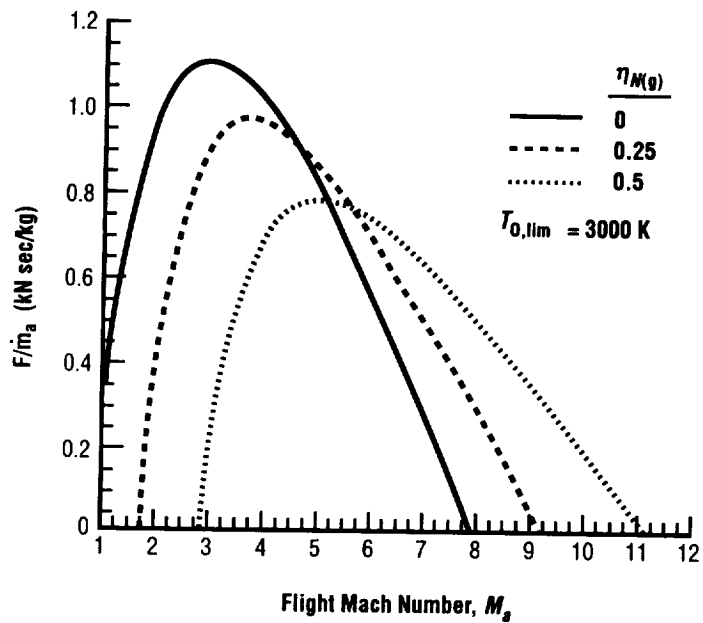


Figure 2. Specific thrust characteristics as a function of flight Mach number for $\eta_{N(g)}=0, 0.25,$ and 0.5 assuming $\eta_{s(g)}=\eta_{s(a)}=0.9$ and $T_{0,lim} = 3000$ K.

3.2 Ramjet Mode Envelope

The combustion optimization attributes can be better appreciated, perhaps, through an inspection of the maximum flight Mach number which can be achieved with MHD-bypass of flow enthalpy while maintaining subsonic combustion conditions. This effect, shown in fig. 3, is demonstrated through solution of eq. (71) assuming a maximum static burner entry temperature of $T_{3,\text{lim}} = 1600$ K. This envelope indicates that the enthalpy extraction ratio in the generator must be extremely high to maintain ramjet mode operation, irrespective of the process efficiencies.

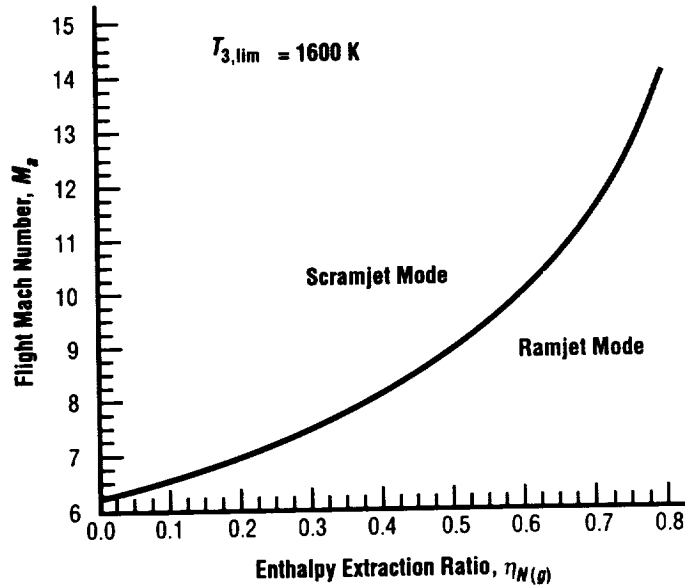


Figure 3. Maximum flight Mach number for maintaining subsonic combustion conditions as a function of the generator enthalpy extraction ratio. Assumes a maximum static burner entry temperature of $T_{3,\text{lim}} = 1600$ K.

3.3 Stream Thrust Analysis

It has not escaped the authors' attention that the present cycle analysis is greatly limited by the assumption of constant specific heat and specific heat ratio throughout the engine flow path. In practice, these parameters change dramatically. The next step in analysis sophistication is to require that these parameters remain constant only within each engine component. This is best done through introduction of the stream thrust function (Sa) defined as

$$Sa = u \left(1 + \frac{RT}{u^2} \right) \quad (72)$$

The stream thrust approach, pioneered by Curran and Craig¹⁴, can be readily generalized for analysis of MHD-bypass engines. For example, it can be shown that the specific thrust of the MHD-bypass engine illustrated in fig. 1 can be expressed in the form¹² (p. 175 of the reference):

$$\frac{F}{\dot{m}_a} = [(1+f)Sa_{10} - Sa_a] - \frac{R_a T_a}{u_a} \left(\frac{A_{10}}{A_a} - 1 \right) \quad (73)$$

where

$$\frac{A_{10}}{A_a} = (1+f) \frac{p_a}{p_{10}} \frac{T_{10}}{T_a} \frac{u_a}{u_{10}} \quad (74)$$

By tracking the evolution of the stream thrust function through the engine, we completed preliminary validation calculations for this analysis methodology. This technique can be utilized to conduct more comprehensive parametric studies and to obtain more realistic estimates of MHD-bypass system performance. The results based on the stream thrust methodology, however, do not alter the basic scientific feasibility findings as deduced from the simplified model.

4. MAJOR TECHNICAL ISSUES

The introduction of plasma/MHD technologies into the propulsion system introduces a host of complex technical and systems integration issues. Most prominent among these is the ionization characteristics and electrical characteristics of the inlet air under various flight conditions and MHD-device performance.

4.1 Air Ionization Considerations

The two major parameters of interest with respect to ionization quality include the electrical conductivity (σ) and the Hall parameter (β). In principle, the degree of MHD interaction depends upon the magnitude of electrical conductivity. However, it is the magnitude of β which can determine the optimal design configuration.

4.1.1 MHD Interaction Parameter

The electrical conductivity is a critical parameter in that it determines the minimum magnetic field strength required for achieving meaningful levels of MHD interaction. For example, lower conductivity implies the need for larger, heavier, and more power-hungry electromagnets. Generally, the manifestation of significant MHD effects requires an interaction parameter on the order of unity. The interaction parameter (Q) is defined as the ratio of MHD forces to the inertial forces in the flow:

$$Q = \frac{\sigma B^2 L}{\rho u} \quad (75)$$

where σ is the electrical conductivity, B is the magnetic induction, L is a characteristic length, ρ is the flow mass density, and u is the flow velocity.

Practically speaking, the product σB^2 should be as high as possible for a given geometry, as defined by L , and for a given flight condition, as defined by the mass flux ρu . Therefore, it is advantageous to utilize the highest achievable electrical conductivity to minimize the required magnet strength.

In general, σ varies in proportion to $T_a/p^{1/2}$ where a is on the order of ten. This implies that plasma/MHD concepts work best at high flight speeds (high temperature) and high altitudes (low pressure). These conditions are ideal for a large portion of the hypersonic flight regime. A question immediately arises, however, as to the minimum flight speed necessary for achieving a naturally occurring plasma capable of sustaining meaningful MHD interaction at reasonable magnetic field strengths.

To address this question, it is of interest to map out the naturally occurring interaction parameter as a function of flight Mach number and altitude, and calculations were performed for equilibrium air behind a normal shock wave. These calculations were carried out with a modified version of the NASA SP-273

chemical equilibrium code in which the plasma electrical transport properties are evaluated according to the methodology of Frost.^{15,16} Results based on the 1976 Standard Atmosphere are shown in fig. 4 assuming a magnetic field strength of 1 T and a characteristic length of 1 m.

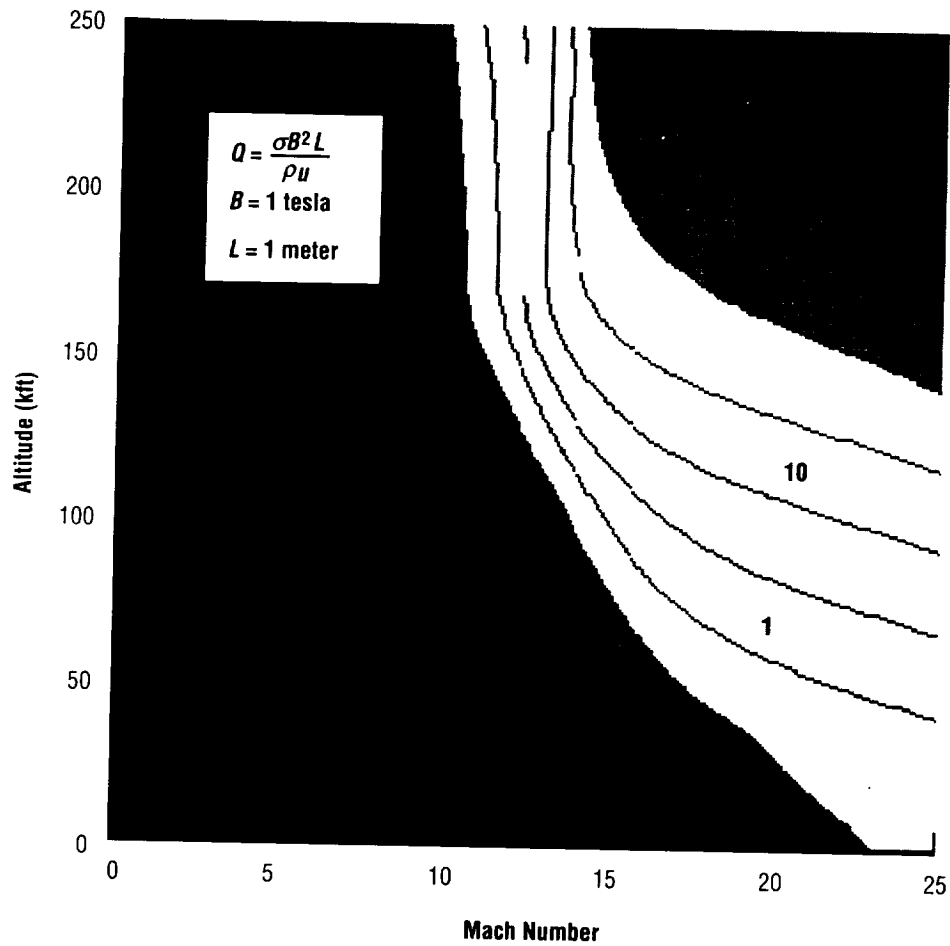


Figure 4. Naturally occurring interaction parameter behind a normal shock as a function of flight Mach number and altitude. Based on 1976 standard atmosphere and equilibrium air with molecular dissociation.

Additional sets of equilibrium air calculations have been performed both with and without cesium seed material. The resulting interaction parameter is shown in fig. 5 as a function of the flight Mach number for fixed altitudes of 100,000 and 125,000 ft. Note that for a concentration of 0.05 percent cesium (molar), significant interaction is available at Mach numbers <10. The dips in the curves are associated with molecular dissociation effects. The fundamental conclusion of these calculations is that equilibrium ionization of inlet air is only practical at mid-to-high hypersonic Mach numbers, say 12 to 18. Application of MHD devices at lower flight speeds will require a power source for inducing nonequilibrium ionization of the air.

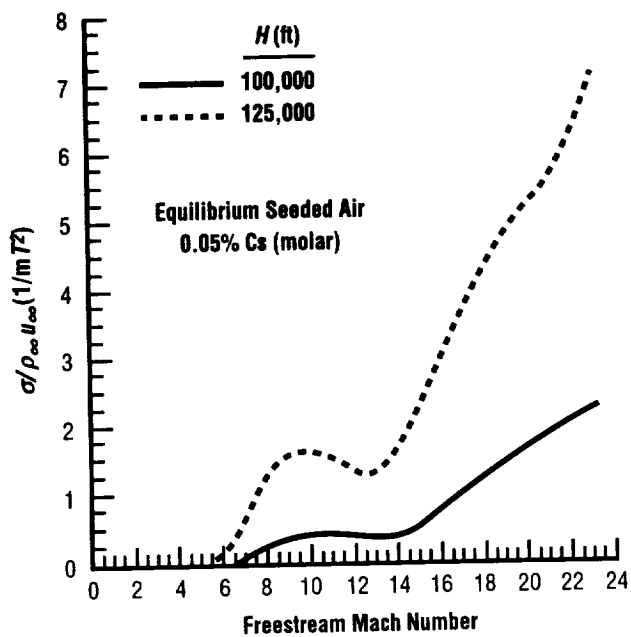
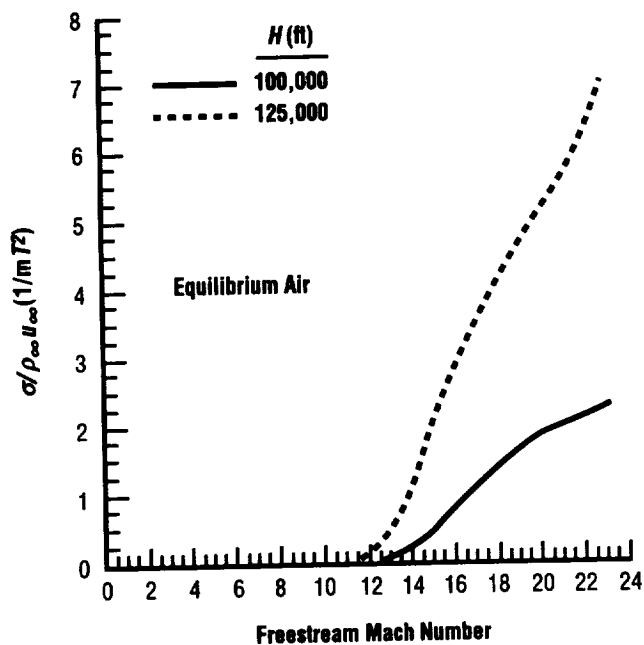


Figure 5. Interaction parameter behind a normal shock as a function of flight Mach number for both unseeded and cesium-seeded equilibrium air. Calculations were performed for fixed altitudes of 100,000 and 125,000 ft.

4.1.2 Hall Parameter

In general, two distinct electric fields are induced when a moving conducting fluid interacts with an applied magnetic induction. The first of these is the Faraday field associated with the bulk motion of charged particles in an applied magnetic field and is defined by the vector $\boldsymbol{\epsilon}_F = \mathbf{u} \times \mathbf{B}$. The second of these is the Hall field which is associated with the electromotive force (emf) generated by the drift velocity \mathbf{w} of the charged particles and is defined by the vector $\boldsymbol{\epsilon}_H = \mathbf{w} \times \mathbf{B}$. Both of these induced fields, in addition to being orthogonal to each other, are orthogonal to the applied magnetic field. Furthermore, these induced fields give rise to two separate components of current density in the conducting fluid which are defined by the following component equations:

$$j_F = \left(\frac{\sigma}{1 + \beta^2} \right) |\mathbf{u} \times \mathbf{B}| \quad (76)$$

and

$$j_H = \left(\frac{\sigma}{1 + \beta^2} \right) \beta |\mathbf{u} \times \mathbf{B}| \quad (77)$$

Thus, the relative magnitude of the Faraday and Hall current components depends upon the absolute magnitude of the Hall parameter. When β exceeds unity, the Hall current becomes greater than the Faraday current. Thus, the magnitude of β determines the appropriate design configuration for any particular application.

Because the Hall parameter increases dramatically with decreasing pressure (i.e., increasing altitude), it is important to assess the anticipated variation in β at the flight conditions of interest. To obtain quantitative predictions for the the Hall parameter under high-altitude hypersonic flight, equilibrium air calculations were performed in which β was deduced assuming an applied magnetic field of 1 T.

The resulting values for the Hall parameter are shown in fig. 6 as a function of the flight Mach number for fixed altitudes of 100,000 and 125,000 ft. One is immediately struck by the large magnitude of β under these conditions, and it is obvious that the results have serious implications with respect to system design configuration.

For a freestream M of 10, for instance, β is ≈ 2 at 100,000 ft and increases to ≈ 7 at 125,000 ft. This means that the Hall current can be as much as 7 times larger than the Faraday current within this flight envelope. For an applied field of 2 T, the Hall parameter would be twice as large. Based on these results, we conclude that the design configuration of plasma/MHD devices must be optimized to take full advantage of the intrinsically large β values.

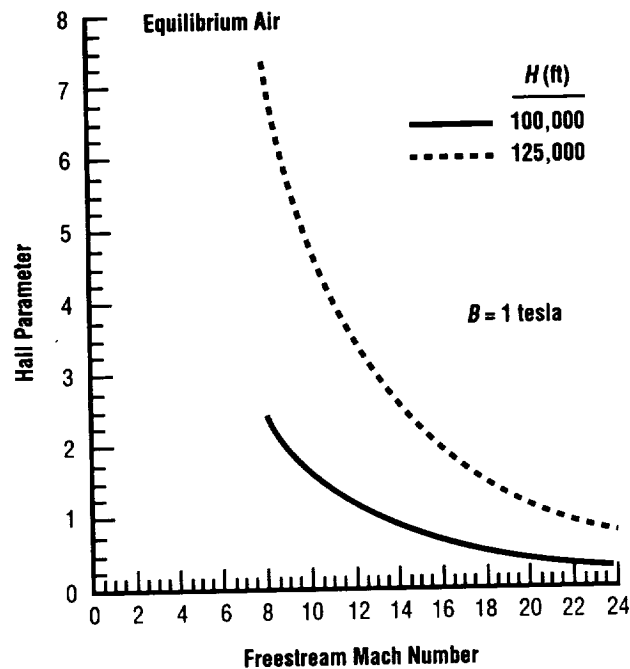


Figure 6. Hall parameter behind a normal shock as a function of flight Mach number for equilibrium air. Calculations were performed for fixed altitudes of 100,000 and 125,000 ft with $B=1$ T.

4.2 MHD Technology Considerations

The technology for MHD generators has matured significantly in recent years and efficiencies are approaching the level needed for practical application. The technology for MHD accelerators, however, is comparatively less developed and there are lingering uncertainties with respect to achievable performance.

A small number of experimental efforts have been conducted over the past 40 yr, but the results have not been conclusively positive.¹⁷⁻²⁴ In many cases, the resulting velocities were much lower than theoretically anticipated. In fact, it has been noted that the observed flow accelerations in these experiments could be associated purely with a thermal heating mechanism rather than true MHD interaction.⁹

In a supersonic flow, for instance, the temperature in the boundary layer near the insulated sidewalls of an MHD device can exceed the temperature in the inviscid core, and the electrical conductivity in the boundary layer will be correspondingly higher. Furthermore, the velocity in the boundary layer is lower than in the inviscid core, and the back emf will be lower. One is therefore led to conclude that there will be less resistance to electric current flow in the boundary layer and that severe leakage currents will occur.

This issue as well as other practical concerns such as maximum axial voltage gradient and generator-accelerator coupling imply that serious research and development must be carried out on the technology of MHD accelerators before the practical feasibility of an MHD-bypass propulsion system can be assessed.

It should also be noted that the development of MHD systems for hypersonic aircraft is currently limited by available enabling technologies for flight-weight magnets and power conditioning units. The primary limitations are related to available magnet field strengths and materials, as well as the intrinsically high weights of magnet materials. In general, superconducting magnet systems are required so that power consumption does not become impractical; unfortunately, this entails the utilization of liquid helium cooling. As an alternative, it has been suggested that it might be possible to employ high-temperature superconductors (HTSC) which can utilize liquid hydrogen as the coolant. This would be desirable for hydrogen-fueled aircraft, however, fabrication techniques and critical current densities for HTSC materials are very limited in their current state of development. Clearly, further research and development are needed on flight-weight magnet enabling technologies for MHD-based aerospace systems.

5. CONCLUSIONS

It has not escaped the authors' attention that our simplified thermodynamic cycle analysis is greatly limited by the assumption of constant stagnation pressure ratios for the various engine components; nevertheless, the analysis does reveal the essential operational benefits of MHD-bypass engines and demonstrates fundamental scientific feasibility. Clearly, bypassing energy around the burner extends the operational Mach number envelope of conventional airbreathing engines, but it is important to note that system performance is extremely sensitive to non-isentropic losses in the MHD devices and that any favorable operational characteristics will disappear if these losses become too large. We conclude that MHD-bypass systems hold significant promise for extending the effective operating range of conventional hypersonic airbreathing engines and believe that the present results justify a more in-depth analysis in which the stagnation pressure ratios become dependent on flight Mach number and the combustion process is modeled more accurately.

In this work, calculations indicated that equilibrium ionization of inlet air is only practical at mid-to-high hypersonic Mach numbers, say 12 to 18, and at altitudes exceeding 100,000 ft. The introduction of ionization seed can relax the Mach number requirement to about 10, but at the expense of increased propellant mass fraction. Calculations also indicate that the Hall Parameter (β) will become significant at these same flight conditions, and it is clear that the design configuration of MHD devices must take into consideration intrinsically high β values.

A review of MHD technology revealed that MHD generator technology is relatively mature whereas MHD accelerator technology suffers from lingering uncertainties with respect to achievable performance. The major concern appears to be the effectiveness of Lorentz force acceleration in MHD devices. In past experiments, for instance, it is suspected that observed flow accelerations may be largely the result of a thermal heating mechanism associated with current leakage in the boundary layer. Further experimental research is needed to resolve this critical issue.

REFERENCES

1. Novichokv, N.: "Space Wings of Russia and the Ukraine," *Echo of the Planet/Aerospace*, Moscow, September 1990.
2. Gurijanov, E.P.; and Harsha, P.T.: "AJAX: New Directions in Hypersonic Technology," *AIAA-96-4609, Seventh Aerospace Planes and Hypersonics Technology Conference*, Norfolk, VA, 1996.
3. Bityurin, V.A.; Lineberry, J.T.; Potebnia, V.G.; Alferov, V.I.; Kuranov, A.L.; and Sheikin, E.G.: "Assessment of Hypersonic MHD Concepts," *AIAA-97-2393, 28th Plasmadynamics and Lasers Conference*, Atlanta, GA, 1997.
4. Bruno, C.; Czysz, P.A.; and Murthy, S.N.B.: "Electro-Magnetic Interactions in Hypersonic Propulsion Systems," *AIAA-97-3389, 33rd Joint Propulsion Conference*, Seattle, WA, 1997.
5. Bruno, C.; and Czysz, P.A.: "An Electro-Magnetic-Chemical Hypersonic Propulsion System," *AIAA-98-1582, Eighth International Space Planes and Hypersonics Systems and Technology Conference*, Norfolk, VA, 1998.
6. Brichkin, D.I.; Kuranov, A.L.; and Sheikin, E.G.: "MHD Technology for Scramjet Control," *AIAA-98-1642, Eighth International Space Planes and Hypersonics Systems and Technology Conference*, Norfolk, VA, 1998.
7. Kuranov, A.L.; and Sheikin, E.G.: "The Potential of MHD Control for Improving Scramjet Performance," *AIAA-99-3535, 30th Plasmadynamics and Lasers Conference*, Norfolk, VA, 1999.
8. Park, C.; Bogdanoff, D.; and Mehta, U.B.: "Theoretical Performance of Frictionless MHD-Bypass Scramjets," *36th JANNAF Combustion Subcommittee/Airbreathing Subcommittee and 18th Propulsion System Hazards Subcommittee Joint Meeting*, Cocoa Beach, FL, October 18-22, 1999.
9. Chase, R.L.; Mehta, U.B.; Bogdanoff, D.W.; Park, C.; Lawrence, S.L.; Aftosmis, M.J.; Macheret, S.; and Shneider, M.: "Comments on an MHD Energy Bypass Engine Powered Spaceliner," *AIAA-99-4975, Ninth Aerospace Planes and Hypersonics Conference*, Norfolk, VA, 1999.
10. Bityurin, V.A.; Lineberry, J.T.; Litchford, R.J.; and Cole, J.W.: "Thermodynamic Analysis of the AJAX Propulsion Concept," *AIAA-2000-0445, 38th AIAA Aerospace Sciences Meeting*, Reno, NV, 2000.
11. Builder, C.H.: "On the Thermodynamic Spectrum of Airbreathing Propulsion," *AIAA-64-243, AIAA First Annual Meeting*, 1964.

12. Heiser, W.H.; and Pratt, D.T. (with Daley, D.H. and Mehta, U.B.), *Hypersonic Airbreathing Propulsion*, AIAA Education Series, American Institute of Aeronautics and Astronautics, Washington, DC, 1994.
13. Hill, P.G.; and Peterson, C.R.: *Mechanics and Thermodynamics of Propulsion*, 2nd ed., Addison-Wesley, Reading, MA, pp. 157–164, 1992.
14. Curran, E.T.; and Craig, R.R.: “The Use of Stream Thrust Concepts for the Approximate Evaluation of Hypersonic Ramjet Engine Performance,” Aero-Propulsion Laboratory, *AFAPL-TR-73-78*, Wright-Patterson AFB, OH, July 1973.
15. Gordon, S.; and McBride, B.J.: “Computer Program for Calculation of Complex Chemical Equilibrium Compositions, Rocket Performance, Incident and Reflected Shocks, and Chapman-Jouguet Detonations,” *NASA SP-273*, 1971.
16. Frost, L.S.: “Conductivity of Seeded Atmospheric Pressure Plasma,” *Journal of Applied Physics*, Vol. 32, No. 10, pp. 2029–2039, 1961.
17. Wood, G.P.; Carter, A.F.; Sabol, A.P.; McFarland, D.R.; and Weaver, W.R.: “Research on Linear Cross Field Accelerators at Langley Research Center, NASA,” in Arc Heaters and MHD Accelerators for Aerodynamic Purposes, *AGARDograph 84*, Part 1, September 1964.
18. Tempelmeyer, K.E.; Whoric, J.M.; Rittenhouse, L.E.; and McKee, M.L.: “Some Characteristics of an Electrical Discharge Transverse to a Supersonic Seeded Nitrogen Plasma Stream with Cold-Copper Electrodes,” *AEDC-TR-65-52*, Arnold Engineering Development Center, Arnold AFB, TN, March 1965.
19. Jedlicka, J.; and Haacker, J.: “Some Experimental Observations on Circulating Currents in a Cross Field Accelerator,” *NASA TM X-67450*, December 1971.
20. Leonard, R.L.: “Experimental Performance of a $j \times B$ Accelerator Augmented Shock Tube,” AVCO Everett Research Laboratory Report 269, May 1967.
21. Rittenhouse, L.E.; Whoric, J.M.; and Pigott, J.C.: “Experimental Results with a Linear Magnetohydrodynamic Accelerator Operated with Water-Cooled Beryllia Magnetic-Field Walls,” *AEDC-TR-70-40*, Arnold Engineering Development Center, Arnold AFB, TN, April 1970.
22. Harris, C.J.; Marston, C.H.; and Warren, W.R.: “MHD Augmented Shock Tunnel Experiments with Unseeded, High Density Air Flows,” *AIAA Journal*, Vol. 13, No. 2, pp. 229–231, February 1974.
23. Love, W.L. and Park C.: “An Experiment on the MHD-Driven Rotating Flow for a Gas-Core Nuclear Rocket,” *AIAA Journal*, Vol. 8, No. 8, pp. 1377–1385, August 1970.
24. Alfeyorov, V.: “A Report on the Status of MHD Hypersonic Ground Test Technology in Russia,” *AIAA-93-3193*, 24th Plasmadynamics and Lasers Conference, 1993.